J. Chem. Sci., Vol. 119, No. 5, September 2007, pp. 533–544.

Reaction mechanism of *O*-acylhydroxamate with cysteine proteases

R SHANKAR and P KOLANDAIVEL*

Department of Physics, Bharathiar University, Coimbatore 641 046
e-mail: ponkvel@hotmail.com

MS received 14 June 2007; accepted 31 July 2007

Abstract. The gas–phase reaction mechanism of *O*-acylhydroxamate with cysteine proteases has been investigated using *ab initio* and density functional theory. On the irreversible process, after breakdown of tetrahedral intermediate (INT1), small 1–2 anionotropic has been formed and rearranged to give stable by-products sulfenamide (P1) and thiocarbamate (P2) with considerable energy loss. While, on the reversible part of this reaction mechanism, intermediate (INT2) breaks down on oxidation, to form a stable product (P3). Topological and AIM analyses have been performed for hydrogen bonded complex in this reaction profile. Intrinsic reaction coordinates [IRC, minimum-energy path (MEP)] calculation connects the transition state between R-INT1, INT1-P1 and INT1-P2. The products P1, P2 and P3 are energetically more stable than the reactant and hence the reaction enthalpy is found to be exothermic.

Keywords. Reaction mechanism; O-acylhydroxamate; cysteine proteases; sulfenamide; thiocarbamate.

1. Introduction

One of the biggest challenges in biochemistry is to understand the nature of enzyme reactions at molecular level.[1] Despite the intensive work over several decades, there is still qualititative understanding of reaction mechanism of enzymes is missing. Proteases are involved in numerous important physiological processes including, digestion, bloodcoagulation, wound healing, fertilization, cell differentiation and growth, cell signalling, and immune response.

Owing to the rapid progress of computational chemistry, understanding of the structure–function relationship of enzyme reactions is becoming an important issue in the theoretical chemistry. The reaction profile of the cysteine proteases inhibitor is also one of the important problems in biochemistry. Proteinases are playing an increasingly important role as a target in the field of drug design.[2] Many diseases or their symptoms originate from a deficiency or an excess of a specific metabolite, which is either a substrate or product of a proteolytic reaction.[4] Thus, modulation of a single enzyme in a sequence of reaction steps can influence the overall effect of a physiological enzyme cascade. Therefore, research on enzyme inhibitors is an important approach in medicinal chemistry.[3] Especially, mechanism-based inhibitor compounds activated during the interaction between target protein and an inhibitor, have potential to lower the side effects of drug administration. Since the reactivity of the inhibitors depends on the catalytic action of the target enzyme on that inhibitor, nonspecific interactions with other protein can be circumvented.[4] Cysteine proteases are ubiquitous enzymes largely distributed in living organisms and are involved in different important metabolic processes and diseases involving various therapeutic fields, such as, cardiovascular, oncology, osteoporosis, and arthritis.

Till now, twenty one families of cysteine proteases have been discovered[5], almost half of them are found in viruses and others are found in bacteria, fungi, protozoa and plants. In mammals, two main groups of cysteine proteases are present: cytosolic calpains and lysosomal cathepsins.[5,6] The cysteine protease inhibitor regulates the action of proteases and plays a significant role in the protection of plants from pest and pathogen attack. The mammalian cysteine proteases are involved in a variety of pathological processes including dysregulated protein turnover such as muscular dystrophy, bone resorption, growth and malignancy of tumors, and myocardial infection.[7,8] Therefore, these enzymes are promising targets for the development of inhibitors as therapeutic agents. Most of them exhibit a peptide segment for recognition by the enzymes and an electrophilic building block for reaction with the cysteine residue of the enzyme's active site as common structural features.

*For correspondence

Nowadays, number of reversible and irreversible cysteine protease inhibitors has been studied. Among them, *O*-acylhydroxamate is the most effective reversible inhibitor of cysteine proteases, and is therefore important in the field of drug design and medicinal chemistry. In addition to this, numerous groups have made important contributions towards the development of cysteine protease inhibitors. These classes of compounds were first described by Fischer and co-workers[9,10] as irreversible inhibitor of serine proteinases, such as α-chymotrypsin and dipeptidyl peptidase. Latter on, they performed NMR study for inhibition of cysteine proteinase, but they have uncovered the reaction profile. Robinson, *et al*[8] have described ^{13}C and ^{15}N NMR characterization of the papain adduct obtained from the *O*-acylhydroxamate having a novel sulfonamide structure. Smith, *et al*[11] have reported that cathepsin B inactivation, the putative tetrahedral intermediate could break down to give turnover products or could produce a stable adduct either by (a) migration of the peptidyl group in a manner similar to a loassen re-arrangement[12] to give a thiocarbamate or by (b) migration of the enzyme thiol group to afford a sulfenamide. Hoffmann and his group[13] have employed quantum mechanical methods which shed new light on the mechanism of the reaction of azathioprine, with cysteine in aqueous solution, in which the first step in the reaction involves the nucleophilic attack of COO^- of cysteine on the C atom of the imidazole ring of azathioprine. This step is followed by subsequent nucleophilic attack of the SH group of cysteine on the C atoms of the imidazole ring, which causes the COO^- group to leave. Thus the cysteine acts in the reaction with azathioprine not only as a reactant, but also as a catalyst of the reaction. Therefore, it can be concluded that biogenic thiol, glutathione or cysteine, facilitate the first and crucial step of azathioprine metabolism, due to the presence of COO^-, SH, and NH_3^+ groups in their molecules.

So for, we know a little about the structural features and binding modes of these propeptides to their target cysteine proteases. A better understanding of these aspects could provide valuable informations for the development of potent and highly selective inhibitors. So, the aim of the present study is to calculate the energy barrier for the reaction mechanism of *O*-acylhydroxamate with cysteine proteases by employing B3LYP and B3PW91 functionals of DFT method with 6-31 + G* basis sets. The local minima are true minima on the potential energy surfaces, and also, transition state structures have also been identified. In addition to that, geometrical parameters for local minima, transition states, and the associated barrier height for all the states have also been determined.

2. Computational details

Geometry of molecules at all stationary points in the potential energy surface have been optimized using B3LYP and B3PW91 functionals of density functional theory implementing 6-31 + G* basis set. Stationary points located have been characterized by computing vibrational frequencies. The nature of the TS has been confirmed not only by the imaginary frequency and also by IRC calculations.[14] Further more, single point energy calculations have been performed at MP2 level of theory for the optimized geometry of B3LYP/6-31 + G* level of theory. The zero-point vibrational energy corrections (ZPVE) have been made for the energy of B3LYP/6-31 + G* and B3PW91/6-31 + G* levels of theory. The topological parameters, like the charge density (ρ) and its second derivative ($\nabla^2\rho$) for bonds are calculated using Bader's atoms in molecules (AIM).[15] The analysis of charge distribution and charge transfer process are performed using NBO 3.1 Program.[16] All these calculations were performed using Gaussian 98 W program.[17] The transition state calculation was performed for intrinsic reaction coordinates (IRC, minimum-energy path (MEP)). The IRC calculation examines the reaction path leading down from a transition structure on a potential energy surface. The calculation starts at the saddle point and follows the reaction in both directions. The IRC calculations definitely connect two minima on the potential energy surface by a path passing through the transition state between them. However, two minima on a potential energy surface may have more than one reaction path connecting them, corresponding to different transition structure through which the reaction passes.[18]

3. Results and discussion

A detailed search of potential energy surface (PES) for the *O*-acylhydroxamate with cysteine proteases reaction mechanism has been performed using DFT method and single point calculations were performed at MP2 level of theory using DFT geometries. The stable structure corresponding to energy minima is identified using frequency analysis and the transi-

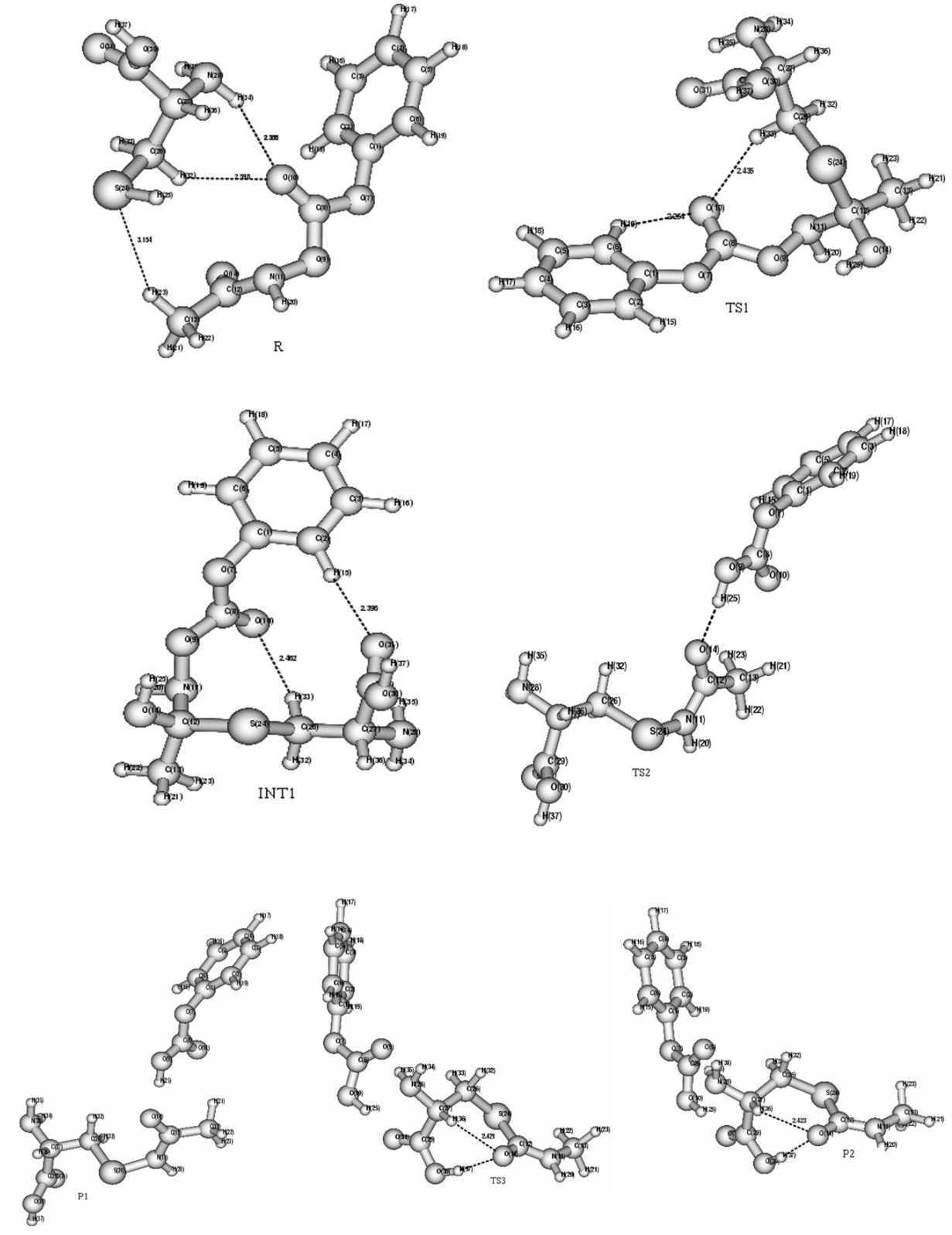

Figure 1. (*contd…*)

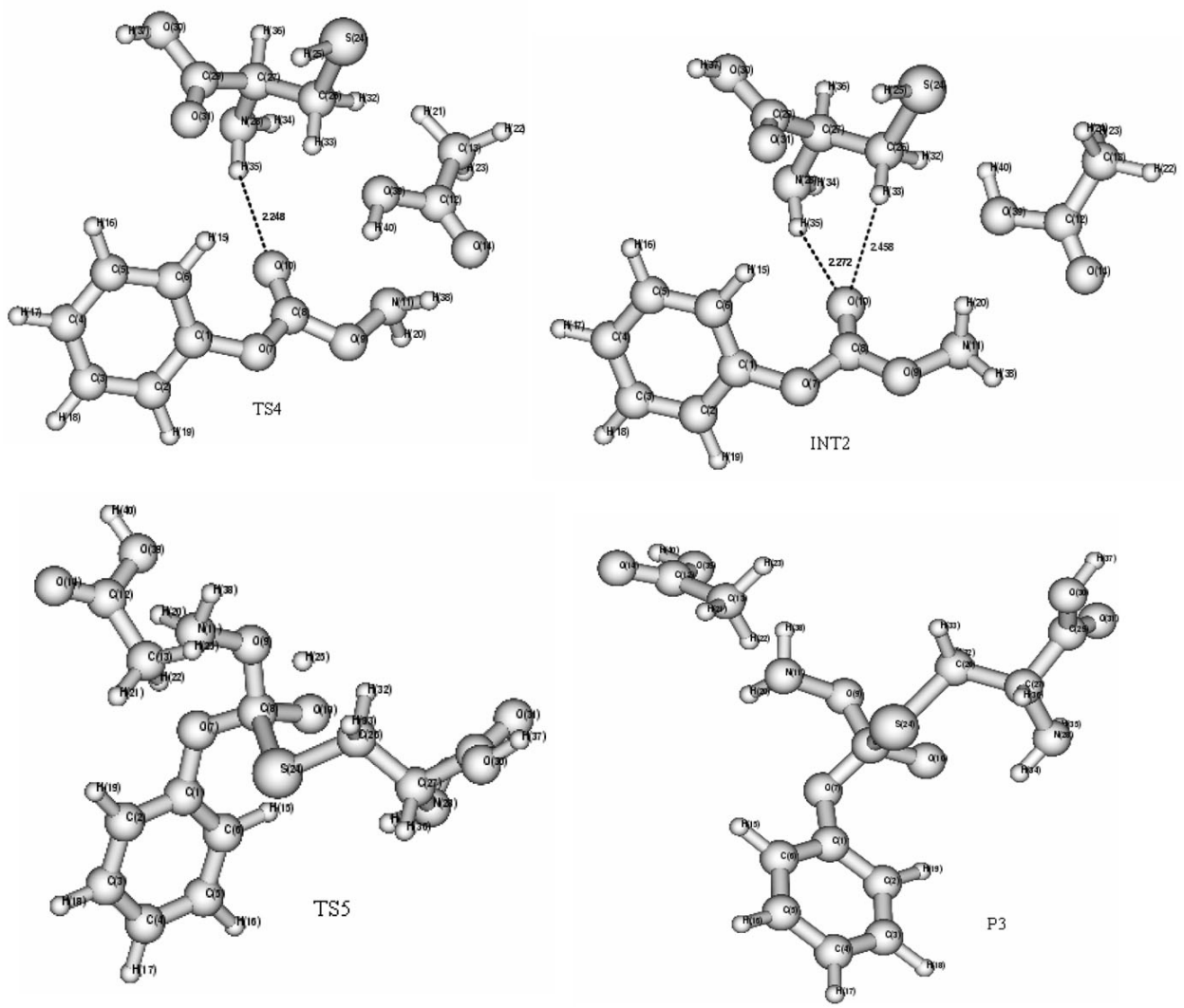

Figure 1. Optimized electronic structures of R, TS1, INT1, TS2, P1, TS3, P2, TS4, INT2, TS5, and P3 for the reaction mechanism of *O*-acylhydroxamate with cysteine proteases.

tion state structure is characterized as first order saddle points by calculating Hessian matrix. The zero point vibrational energy corrections have been made in order to predict the accurate and reliable energy. The electronic structures of the reactant R, transition states (TS1, TS2, TS3, TS4, and TS5), the intermediates (INT1, and INT2) and products (P1, P2 and P3) which are depicted in figure 1 and the corresponding geometrical parameters are presented in tables 1–3. The (IRC) calculations connect the transition state between R-INT1, INT1-P1 and INT1-P2, but it fails to converge at transition state between the INT1-INT2 and INT2-P3.

3.1 *Formation of the tetrahedral intermediates (INT1)*

The reaction mechanisms of *O*-acylhydroxamate with cysteine proteases have been carried out using high level *ab initio* and DFT theories. The calculated frequencies show that tetrahedral intermediate (INT1) is in local minima on the potential energy surface (PES), and it is formed through the transition state (TS1). During the formation of tetrahedral intermediate (INT1), an intermolecular transition has occurred, in which, the protonated active cysteine molecule (hydrogen atom (H_{25}) of active thiol group of the

Table 1. Selected optimized geometrical parameters (bond length *r* in Å, bond angle A and torsional angle D in degrees), formation of product (P1) on reaction mechanism of *O*-acylhydroxamate with cysteine, calculated using DFT methods implementing 6-31 + G* basis set.

	R		TS1		INT1		TS2		P1	
Structures	B3PW91	B3LYP	B3PW91	B3LYP	B3PW91	B3LYP	B3LYP	B3PW91	B3LYP	B3PW91
r (1, 2)	1·392	1·392	1·397	1·394	1·392	1·390	1·393	1·393	1·393	1·392
r (1, 7)	1·410	1·410	1·404	1·396	1·408	1·401	1·397	1·397	1·398	1·391
r (7, 8)	1·340	1·340	1·342	1·338	1·346	1·343	1·358	1·358	1·357	1·353
r (8, 9)	1·369	1·369	1·369	1·364	1·368	1·363	1·325	1·326	1·325	1·320
r (8, 10)	1·202	1·202	1·202	1·199	1·200	1·198	1·215	1·215	1·216	1·214
r (11, 12)	1·399	1·399	1·468	1·462	1·465	1·459	1·372	1·372	1·372	1·368
r (12, 13)	1·514	1·514	1·525	1·520	1·525	1·520	1·513	1·513	1·513	1·507
r (13, 23)	1·096	1·096	1·092	1·092	1·092	1·093	1·094	1·094	1·094	1·094
r(12, 14)	1·216	1·216	1·409	1·403	1·409	1·403	1·232	1·232	1·233	1·230
r (12, 24)	–	–	1·866	1·854	1·868	1·856	–	–	–	–
r (24, 26)	1·847	1·847	1·848	1·833	1·847	1·832	1·848	1·847	1·848	1·844
r (24, 11)	–	–	–	–	–	–	1·722	1·722	1·710	1·710
r (27, 29)	1·526	1·526	1·527	1·522	1·527	1·523	1·528	1·528	1·528	1·524
r (29, 30)	1·351	1·350	1·351	1·345	1·349	1·343	1·349	1·349	1·349	1·343
r (29, 31)	1·214	1·214	1·212	1·211	1·213	1·212	1·213	1·213	1·213	1·211
A(1, 2, 3)	118·499	118·513	119·405	119·456	118·223	118·891	119·212	119·212	119·213	119·213
A(1, 7, 8)	117·613	117·374	124·085	123·988	118·900	118·633	119·653	119·653	119·774	119·629
A(7, 8, 9)	105·127	105·027	104·136	104·057	104·678	104·584	107·892	107·892	107·986	107·906
A(7, 8, 10)	128·172	128·278	129·008	129·147	128·144	128·185	125·448–	125·448	125·329	125·126
A(9, 11, 12)	115·328	115·607	107·902	107·818	108·004	107·894	–	–	–	–
A(11, 12, 13)	121·833	121·862	113·402	113·524	113·700	113·802	121·230	115·719	116·224	115·899
A(11, 12, 14)	113·349	113·303	107·265	107·269	107·159	107·178	115·719	121·230	127·557	121·257
A(26, 27, 28)	113·461	113·455	113·054	113·044	113·225	113·244	113·545	113·545	113·475	109·972
A(24, 26, 27)	114·746	114·905	111·637	111·616	111·254	111·249	111·018	111·018	111·136	111·136
A(28, 27, 29)	106·838	106·908	106·679	106·671	106·508	106·560	106·340	106·340	106·384	106·023
A(30, 29, 31)	122·929	123·036	123·194	123·283	123·007	123·173	123·418	123·418	123·413	123·497
A(24, 12, 13)	–	–	112·805	112·782	112·429	112·417	–	–	–	–
A(26, 24, 11)	–	–	–	–	–	–	100·943	100·943	100·836	100·957
D(24, 26, 27, 28)	–175·947	–176·798	176·581	177·060	–179·904	–179·863	173·349	173·447	173·349	173·777
D(24, 26, 27, 29)	–64·003	–63·328	–63·913	–63·566	–60·338	–46·782	–67·483	–67·371	–67·483	–67·254
D(26, 27, 29, 30)	121·528	119·978	103·491	103·029	111·823	110·526	117·541	116·712	117·541	117·691

cysteine molecule) is deprotonated to form a stable INT1. During the deprotonation, the hydrogen atom (H_{25}) of active thiol group is directed to the oxygen atom (O_{14}) and binds to acylhydroximate of peptide residue end. Likewise, similar process is found to occur in the enzymatic activity, where, the deprotonated cysteine enzyme S^- ions bind to the stronger electrophile (positively charged) acylhydroximate chiral carbon atom C_{20} of the peptide residue end. Also, due to the proton transfer, C_{12}–$O_{14}\pi$ bond has been cleaved and a σ bond is formed, the bond length between C_{12}–O_{14} gets elongated and the elongation values are found to be 0·193 and 0·187 Å at B3LYP and B3PW91/6-31 + G* levels of theory respectively, which has been confirmed not only by the elongation of the C_{12}–O_{14} bond but also by the low electron density in AIM analysis. Moreover, bond between C_{12}–S_{24} atoms is not strong, so it can be easily cleaved and rearranged to form a stable product where the electron density and laplacian density of C_{12}–S_{24} bond are found to be 0·169 and –0·253 a.u., which confirms the weak nature of the bond at TS1. The topological and AIM analyses of the hydrogen bonded network in the *O*-acylhydroxamate with cysteine proteases reaction mechanism have been shown in the tables 4 and 5. It is quite interesting to note that intermolecular weak hydrogen bonded network between the reactants *O*-acyl hydroxamates and protonated cysteine molecules are found between N_{28}–H_{34}…O_4, O_{26}–H_{32}…O_{10} and C_{13}–H_{23}…S_{24} atoms. Generally for hydrogen bonded complex, the electron density (ρ) and laplacian of electron density ($\nabla^2\rho$) are in the range of 0·002–0·34 and 0·016–0·139 a.u., respectively.[19,20] In the present study, the

Table 2. Selected optimized geometrical parameters (bond length *r* in Å, bond angle A and torsional angle *D* in degrees), formation of product (P2) on reaction mechanism of *O*-acylhydroxamate with cysteine, calculated using DFT methods implementing 6-31 + G* basis set.

	R		TS1		INT1		TS3		P1	
Structures	B3LYP	B3PW91	B3LYP	B3PW91	B3LYP	B3PW91	B3LYP	B3PW91	B3LYP	B3PW91
r (1,2)	1·392	1·392	1·397	1·395	1·393	1·390	1·392	1·390	1·393	1·392
r (1,7)	1·410	1·410	1·403	1·396	1·408	1·401	1·400	1·393	1·391	1·391
r (7,8)	1·340	1·340	1·342	1·338	1·346	1·343	1·353	1·350	1·357	1·353
r (8,9)	1·369	1·369	1·369	1·364	1·368	1·363	1·220	1·218	1·325	1·320
r (8,10)	1·202	1·202	1·202	1·200	1·200	1·198	1·320	1·315	1·216	1·214
r (9,11)	1·406	1·406	1·442	1·428	1·441	1·427	–	–	–	–
r (11,12)	1·399	1·399	1·468	1·462	1·465	1·459	1·353	1·350	1·372	1·368
r (12,14)	1·216	1·216	1·409	1·403	1·409	1·403	1·239	1·237	1·233	1·230
r (24,26)	1·847	1·847	1·848	1·833	1·847	1·832	1·852	1·836	1·833	1·834
r (27,36)	1·094	1·095	1·095	1·095	1·094	1·095	1·091	1·094	1·091	1·092
r (26,27)	1·542	1·542	1·550	1·545	1·547	1·542	1·557	1·552	1·545	1·540
r (27,28)	1·464	1·464	1·463	1·456	1·464	1·457	1·454	1·447	1·464	1·457
r (29,30)	1·351	1·351	1·351	1·345	1·348	1·343	1·333	1·327	1·349	1·343
r (29,31)	1·214	1·213	1·212	1·211	1·214	1·212	1·219	1·217	1·213	1·211
r (12,24)	–	–	1·866	1·854	1·868	1·856	1·804	1·792	1·802	1·792
r (30,37)	0·977	0·975	0·977	0·975	0·977	0·975	0·989	0·989	0·989	0·989
A(1,7,8)	117·613	117·374	124·085	123·988	118·900	118·633	119·147	118·798	119·217	118·941
A(7,8,9)	105·127	105·027	104·136	104·057	104·678	104·584	124·874	124·757	124·897	124·799
A(7,8,10)	128·172	128·278	129·008	129·147	128·144	128·185	108·483	108·456	108·475	108·430
A(11,12,14)	113·349	113·303	107·265	107·269	107·159	107·178	121·271	121·298	121·892	121·910
A(26,27,28)	113·461	113·455	113·054	113·044	113·225	113·244	111·626	111·659	111·646	111·703
A(24,26,27)	114·040	114·905	111·637	111·616	111·254	111·249	121·563	121·698	121·519	121·622
A(28,27,29)	122·929	123·036	123·194	123·283	123·007	123·173	119·938	120·038	119·925	120·038
A(30,29,31)	–	–	110·393	110·249	110·420	110·245	116·108	116·005	114·768	114·684
A(24,12,13)	–	–	105·967	105·933	105·999	105·997	122·532	122·609	123·290	123·357
A(24,12,11)	–	–	110·393	110·249	110·420	110·245	116·108	116·005	114·768	114·684
A (24,12,14)	–	–	105·967	105·933	105·999	105·997	122·532	122·609	123·290	123·357
D(12,24,26)	–	–	102·860	102·763	102·830	102·680	103·043	102·853	103·304	103·113
D(11,12,24,26)	–	–	–49·575	–50·318	–46·782	–46·782	–157·569	–157·550	–158·302	–157·943
D(14,12,24,26)	–	–	–172·787	–172·787	–170·369	–170·369	25·840	25·840	24·216	24·548
D(24,26,27,29)	–63·328	–	–63·679	–63·566	–60·679	–60·679	–42·993	–42·993	–43·376	–42·867
D(24,26,27,28)	176·798	–	177·060	177·060	179·863	179·863	–165·979	–165·979	–166·306	–165·837

values of ρ and $\nabla^2\rho$ are found to vary from 0·004 to 0·117 and 0·012–0·135 au, respectively. So the above values indicate that all the complexes are having intermolecular hydrogen bonds.

During the formation of tetrahedral intermediate INT1, the entire intermolecular hydrogen bonded networks N_{28}–H_{34}…O_{11}, O_{26}–H_{32}…O_{10} and C_{13}–H_{23}…S_{24} of the reactants are cleaved in order to form a new intramolecular hydrogen bonded bridges between C_2–H_{15}…O_{31} and C_{26}–H_3…O_{10} atoms. As we know that hydrogen bonds are formed due to the charge transfer from the proton acceptor to proton donor, the amount of charge transfer is significant for the elongation and contraction of X–H bond. For each donor and acceptor the stabilization energy E is associated with *i*–*j* delocalization which is given by the following equation

$$E^{(2)} = \Delta E_{ij} = q_i \frac{F^2(i, j)}{\varepsilon_j - \varepsilon_i}.$$

where, q_i the *i*th donor orbital occupancy, ε_j, ε_i are diagonal elements (orbital energies) and $F(i, j)$ is off diagonal elements respectively, associated with NBO Fock matrix.

Obviously, in INT1, the large stabilization energy of 2·07 kcal /mol for C_2–H_{15}…O_3 shows the maximum stability, when compared with the reactant hydrogen bonded network. But, the order of the molecular stability shows that the tetrahedral intermediate has

Table 3. Selected optimized geometrical parameters (bond length *r* in Å, bond angle A and torsional angle *D* in degrees), formation of product (P3) on reaction mechanism of *O*-acylhydroxamate with cysteine, calculated using DFT methods implementing 6-31 + G* basis set.

	R		TS1		INT1		TS4		INT2		TS5		P3	
	B3LYP	B3PW91	B3LYP	B3PW91	B3LYP	B3PW91	B3LYP	B3PW91	B3LYP	B3PW91	B3LYP	B3PW91	B3LYP	B3PW91
r (1,2)	1·392	1·392	1·397	1·395	1·393	1·390	1·392	1·392	1·392	1·390	1·393	1·392	1·395	1·393
r (1,7)	1·410	1·410	1·403	1·396	1·408	1·401	1·410	1·410	1·403	1·396	1·402	1·394	1·396	1·392
r (8,9)	1·369	1·369	1·369	1·364	1·368	1·363	1·363	1·363	1·338	1·335	1·392	1·392	1·391	1·391
r (8,10)	1·202	1·202	1·202	1·200	1·200	1·198	1·206	1·206	1·211	1·208	1·407	1·400	1·395	1·385
r (11,12)	1·399	1·399	1·468	1·462	1·465	1·459	–	–	–	–	–	–	–	–
r (12,13)	1·514	1·514	1·525	1·520	1·525	1·520	1·510	1·510	–	–	–	–	1·503	1·499
r (12,14)	1·216	1·216	1·410	1·403	1·409	1·403	1·222	1·223	1·210	1·209	1·211	1·210	1·211	1·209
r (24,26)	1·847	1·847	1·848	1·833	1·847	1·832	1·845	1·845	1·852	1·837	1·840	1·843	1·839	1·826
r (26,27)	1·542	1·542	1·550	1·545	1·547	1·542	1·539	1·539	1·536	1·531	1·558	1·554	1·558	1·553
r (27,29)	1·526	1·526	1·527	1·522	1·527	1·523	1·527	1·527	1·530	1·525	1·529	1·526	1·523	1·519
r (27,28)	1·464	1·457	1·463	1·456	1·464	1·457	1·464	1·464	1·465	1·458	1·464	1·459	1·453	1·447
r (24,25)	–	–	–	–	–	–	1·351	1·351	1·350	1·349	–	–	–	–
r (29,31)	1·214	1·214	1·212	1·211	1·214	1·212	1·217	1·217	1·217	1·215	1·218	1·216	1·212	1·212
r (12,24)	–	–	1·866	1·854	1·868	1·856	–	–	–	–	–	–	–	–
r (24,8)	–	–	–	–	–	–	–	–	–	–	1·854	1·850	1·843	1·842
A(1,2,3)	118·499	118·513	119·405	119·456	118·223	118·891	118·846	118·846	119·023	119·048	119·023	119·200	119·504	119·513
A(1,7,8)	117·613	117·374	124·085	123·988	118·900	118·633	120·110	120·110	119·411	118·921	120·133	121·233	121·243	121·246
A(7,8,9)	105·127	105·027	104·136	104·057	104·678	104·584	105·345	105·345	106·292	106·114	105·543	105·225	105·834	105·924
A(7,8,10)	128·172	128·278	129·008	129·147	128·144	128·185	128·329	128·329	126·891	126·911	113·682	112·955	113·520	113·675
A(8,9,11)	112·525	112·341	112·893	112·744	112·708	112·610	111·552	111·552	112·322	112·223	112·125	112·102	112·084	111·937
A(11,12,13)	121·833	121·862	113·402	113·524	113·700	113·802	–	–	–	–	–	–	–	–
A(11,12,14)	113·349	113·303	107·265	107·269	107·159	107·178	–	–	–	–	–	–	–	–
A(26,27,28)	113·461	113·455	113·054	113·044	113·225	113·244	112·948	113·888	112·726	112·825	116·380	116·350	116·380	116·192
A(24,26,27)	117·040	116·905	111·637	111·616	111·254	111·249	115·278	115·274	115·588	115·496	112·252	112·032	112·020	111·922
A(26,27,29)	110·584	110·260	110·537	110·373	110·769	110·504	110·948	110·948	111·459	111·268	106·902	106·660	106·882	106·709
A(30,29,31)	122·929	123·036	123·194	123·283	123·007	123·173	122·608	112·608	122·726	122·808	122·708	122·792	122·717	122·820
D(24,26,27,29)	–175·947	–176·798	–176·58	–177·06	–179·904	–179·863	–157·28	–155·555	–179·98	–179·871	–175·713	–176·110	–176·073	–176·866
D(24,26,27,28)	–64·003	–63·328	–63·913	–63·566	–60·338	–66·782	–64·694	–64·694	–60·451	–60·096	–87·182	–87·202	–65·187	–61·877
D(26,27,29,30)	121·528	119·978	103·491	103·029	111·823	110·526	137·882	137·882	147·909	151·056	157·932	156·552	158·032	157·632

Table 4. Occupation number of the X–H, Z–X bonds of the acceptor , the lone pairs of the acceptor atom and their corresponding energies (a.u), hydrogen bond length H…Y in Å and stabilization energy (in kcal/mol) of the interaction between lone pairs of acceptor atoms the anti-bonding orbitals are calculated using B3LYP theory at 6-31 + G* basis set.

		Donor				Acceptor		
System	Bonding	r(Z–X)	σ^*(Z–X)	r(X–H)	σ^*(X–H)	n(Y)	H….Y	E(2)$n(y) \rightarrow \sigma^*$(X – H)
R	N_{28}–H_{34}…O_{10}	–	–	1·019	0·011	1·970	2·356	1·80
	S_{24}–C_{26}–H_{32}…O_{10}	1·847	0·023	1·092	0·018	1·970	2·596	0·73
	C_{12}–C_{13}–H_{23}…S_{24}	1·514	0·054	1·097	0·010	1·994	3·154	1·48
TS1	S_{24}–C_{26}–H_{33}…O_{10}	1·848	0·028	1·092	0·023	1·971	2·435	0·84
	C_5–C_6–H_{19}…O_{10}	1·310	0·015	1·086	0·015	1·813	2·254	1·38
INT1	C_1–C_2–H_{15}…O_{31}	1·393	0·026	1·085	0·016	1·973	2·396	2·07
	S_{24}–C_{26}–H_{33}…O_{10}	1·847	0·028	1·092	0·022	1·972	2·462	0·74
TS3	N_{28}–C_{27}–H_{36}…O_{14}	1·454	0·015	1·091	0·019	1·958	2·421	0·51
	O_{30}–H_{37}…O_{14}	–	–	0·989	0·046	1·958	1·815	7·44
P2	N_{28}–C_{27}–H_{36}…O_{14}	1·454	0·015	1·091	0·019	1·840	2·423	0·52
	O_{30}–H_{37}…O_{14}	–	–	0·989	0·046	1·958	1·816	7·38
TS4	N_{28}–H_{35}…O_{10}	–	–	1·020	0·013	1·969	2·248	3·27
INT2	S_{24}–C_6–H_{33}…O_{10}	1·852	0·025	1·091	0·019	1·969	2·458	1·02
	N_{28}–H_{35}…O_{10}	–	–	1·02	0·013	1·969	2·272	2·90

Table 5. Topological analysis of electron density (ρ), laplacian density ($\nabla^2\rho$) and ellipticity (ε) and hydrogen bond length R (Å) calculated using B3LYP method at 6-31 + G* basis set.

Bonding		R (Å)	ρ(a.u.)	$\nabla^2\rho$ (a.u.)	ε(a.u.)
R	N_{28}–H_{34}…O_{10}	2·356	0·0097	0·0384	0·0692
	S_{24}–C_{26}–H_{32}…O_{10}	2·596	0·0069	0·0261	0·0515
	C_{12}–C_{13}–H_{23}…S_{24}	3·154	0·0050	0·0147	0·0445
TS1	S_{24}–C_{26}–H_{33}…O_{10}	2·435	0·0090	0·0335	0·0600
	C_5–C_6–H_{19}…O_{10}	2·254	0·0174	0·0658	0·233
INT1	C_1–C_2–H_{15}…O_{31}	2·396	0·0091	0·0348	0·0718
	S_{24}–C_{26}–H_{33}…O_{10}	2·462	0·0091	0·0328	0·0660
TS3	N_{28}–C_{27}–H_{36}…O_{14}	2·421	0·0130	0·0478	0·2125
	O_{30}–H_{37}…O_{14}	1·815	0·0347	0·1107	0·0334
P2	N_{28}–C_{27}–H_{36}…O_{14}	2·423	0·0130	0·0475	0·2055
	O_{30}–H_{37}…O_{14}	1·816	0·0346	0·1317	0·0102
TS4	N_{28}–H_{35}…O_{10}	2·248	0·0118	0·0466	0·0673
INT2	S_{24}–C_6–H_{33}…O_{10}	1·969	0·0092	0·0335	0·0279
	N_{28}–H_{35}…O_{10}	1·969	0·0115	0·0445	0·0570

less stability than the reactant. This may be due to cleavage of large number of hydrogen bonded networks in INT1. At TS1, the bond lengths N_{11}–C_{12}, C_{12}–C_{13}, C_{12}–O_{14} gets elongated and the elongation values are found to be 0·068, 0·010 and 0·193 Å respectively.

In TS1, the intramolecular hydrogen bonded networks C_{26}–H_3…O_{10}, C_6–H_{19}…O_{10} have been observed. The stabilization energies of C_{26}–H_3…O_{10} and C_6–H_{19}…O_{10} are found to be 0·84 and 1·38 kcal/mol respectively, but this hydrogen bonded bridge has been cleaved during the formation of tetrahedral intermediate INT1. The (IRC) calculations connect the transition state between the reactant and tetrahedral intermediate INT1. The energy barrier between the reactant to transition state TS1 is found be 15·24, 12·05 and 4·07 kcal/mol at B3LYP/6-31 + G*, B3PW91/6-31 + G* and MP2//B3LYP/6-31 + G* levels of theory, respectively. During the formation of the tetrahedral intermediate INT1, N_{11}–C_{12} and

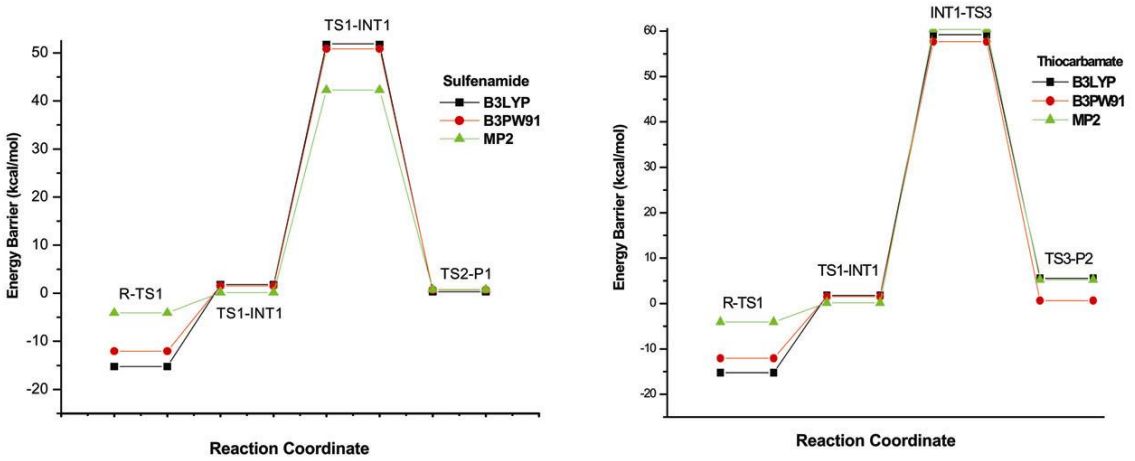

Figure 2. Calculated energy barrier (kcal/mol) for the formation of products P1 and P2 DFT and *ab initio* methods implementing 6-31 + G* basis set.

C_{12}–O_{14} bonds get shortened and their respective values are given in table 1. The energy barrier between TS1 and INT1 is found to be 1·79, 1·53 and 0·12 kcal/mol at B3LYP/6-31 + G*, B3PW91/6-31 + G* and MP2//B3LYP/6-31 + G* levels of theory respectively. In spite of the structural resemblance between TS1 and INT1, the internal geometry shows some small discrepancies. The INT1 structure is found to be less stable than the reactant which is indicated by the reaction barrier of –13·45 and –10·51 kcal/mol calculated at B3LYP/6-31 + G* and B3PW91/6-31 + G* levels of theory.

3.2 *Breakdown of the tetrahedral intermediate (INT1)*

The stable tetrahedral intermediate INT1 is a bridge between the reactant and product on the cysteine proteases inhibitor reaction profile. The previous calculations by Perakyla *et al*[21] were based on the assumption that the transition state structures during the formation/breakdown of the tetrahedral intermediate are very similar to that of the tetrahedral intermediate.[21–24] In the present calculation, the transition state structures TS1, TS2, TS3, and TS4 are found to be similar to that of the INT1, INT2, P1, P2, P3 and reactants. Additionally during the breakdown of the stable tetrahedral intermediate INT1, two stable by-products sulfenamide and thiocarbamate have been formed through TS2 and TS3 on the reaction profile of the cysteine proteases reaction mechanisms.

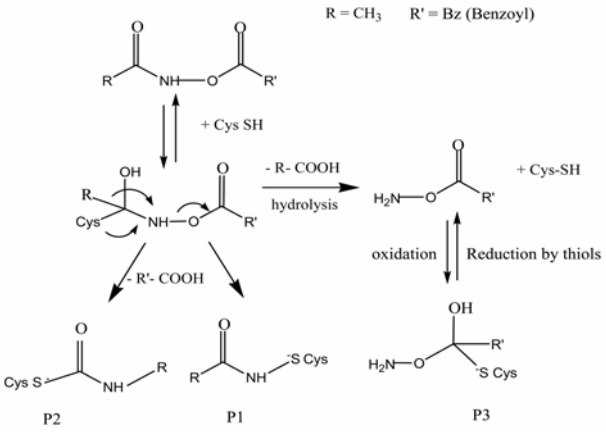

Scheme 1. Proposed mechanisms of inhibition of cysteine proteases by O–acylhydroxamate.

3.2a *Formation of sulfenamide (P1):* It is also one of the by-products and very strong inhibitor of cysteine proteases reaction mechanism profile, where the sulfenamide P1 is formed through the transition state TS2, and again the bond between O_{14}–H_{25} atoms in the tetrahedral intermediate INT1 is cleaved, therefore, the σ bond between O_{14}–C_{12} atoms changes to the π bond character. In the mean time, enzymatic cysteine proteases ions are cleaved from the acylhydroximate chiral carbon atom C_{12} and strongly bind to the strong electrophile N_{11} nitrogen atom of the *O*-acylhydroxamate. Due to the electrophilic attack of cysteine ions, bond between N_{11}–O_9 atoms is cleaved. During the formation of TS2, the bond length of S_{24}–C_{26} atoms gets elongated by 0·015 Å at

B3PW91/6-31 + G* level of theory. At the same time, the bond lengths C_8–N_{11}, N_{11}–C_{12} and C_{12}–O_{14} are shortened by 0·168, 0·086 and 0·170 Å at B3LYP/6-31 + G* level of theory respectively. The IRC calculation connects the transition state between the tetrahedral intermediate INT1 and the product P1. The energy barrier for formation of the transition state structure TS2 is calculated to be 51·86, 50·81 and 42·23 kcal/mol at B3LYP/6-31 + G*, B3PW91/6-31 + G*, and MP2//B3LYP/6-31 + G*, levels of theory respectively and also, during the formation of TS2, the entire intramolecular hydrogen bonds network have been cleaved. The energy barrier on each steps of the reaction profile of the thiocarbamate P1 is calculated and the results are presented in figure 1. The energy barrier between the TS2 and product P1 is found to be 0·32, 0·73 and 0·75 kcal/mol at B3LYP/6-31 + G*, B3PW91/6-31 + G* and MP2//B3LYP 6-31 + G* levels of theory respectively. Due to the occurrence of low energy barrier between TS2 and the product P1, the TS2 was easily re-arranged to form a stable product P1. Also, the product P1 was more stable than the reactant, and the reaction energy was found to be 38·73, 39·57 and 39·53 kcal/mol at B3LYP/6-31 + G*, B3PW91/6-31 + G* and MP2//B3LYP/6-31 + G* levels of theory respectively. Additionally, the negative values of the reaction energies indicate that, the overall reaction profile of P1 is found to be exothermic.

During the formation of sulfenamide P1, the bond length between S_{24}–N_{11} atoms is shortened by 0·115 and 0·011 Å at B3LYP/6-31 + G* and B3PW91/6-31 + G* levels of theory when compared with TS2 and INT1 states. The stability of the S_{24}–N_{11} bond has been calculated by electron density and laplacian density using AIM analysis. The electron density and laplacian density of S_{24}–N_{11} bond are found to be 0·186, and –0·167 a.u. at B3LYP/6-31 + G* level of theory, which shows a strong covalent nature of the bonding. This result confirms the inhibiting nature of the product P1.

3.2b *Formation of thiocarbamate P2:* On the irreversible reaction mechanism of cysteine proteases with *O*-acylhydroxamate, thiocarbamate P2 is also one of the byproduct. The calculated frequency for thiocarbamate P2 at the above mentioned levels of theory confirmed that the structures are on real local minima on the potential energy surface (PES), whereas, the product P2 is formed through the transition state TS3. The numerical frequency calculation shows that TS3 has one imaginary frequency. During the formation of transition state TS3, the entire intra-molecular hydrogen bonded networks in the tetrahedral intermediate INT1 have been cleaved, to form new hydrogen bonded networks C_{27}–H_{36}…O_{14} and O_{30}–H_{37}…O_{14} in TS3, where the stabilization energies of the C_{27}–H_{36}…O_{14} and O_{30}–H_{37}…O_{14} are found to be 7·44 and 0·51 kcal/mol at B3LYP/6-31 + G* level of theory. The IRC calculations connect the transition state between the tetrahedral intermediate INT1 and the product P2. The energy barrier on each steps of the reaction profile of the sulfenamide P2 is calculated and the results are presented in figure 2. The energy barrier between the tetrahedral intermediate INT1 and transition state TS3 is found to be 59·20, 57·65 and 60·36 kcal/mol at B3LYP/6-31 + G*, B3PW91/6-31 + G*1 and MP2//B3LYP/6-31 + G* levels of theory. In TS3, the bond lengths of C_{12}–O_{14}, C_{12}–S_{24} and N_{11}–C_{12} get contracted by 0·170, 0·064 and 0·111 Å respectively at B3LYP/6-31 + G* level of theory. Obviously at the same time, bond length of C_{26}–C_{27} gets elongated by 0·016 and 0·015 Å at B3LYP/6-31 + G* and B3PW91/6-31 + G* levels of theory. The energy barrier between TS3 and product P2 is found to be 5·52, 0·65 and 5·25 kcal/mol at the above levels of theory. Also, during the formation of product P2, bond between deprotonated cysteine ions and *O*-acylhydroxamate, N_{12}–S_{24} further contracts to form a strong covalent bond. In addition to that, the electron density between N_{12}–S_{24} atoms also confirms the strong covalent nature. The product P2 is more stable than the reactant and the energy barrier between the reactant and product P2 is found to be 51·26, 47·75 and 45·98 kcal/mol at B3LYP/6-31 + G*, B3PW91/6-31 + G* and MP2//B3LYP/6-31 + G* levels of theory respectively. Owing to the occurrence of the heavy energy barrier, the formation of product P2 is less favoured than product P1 on this reaction profile. The product P2 is found to be more stable than the reactant R; hence, its overall reaction profile of P2 is found to be exothermic nature.

3.3 *Formation and breakdown of INT2*

The breakdown of the tetrahedral intermediate INT1 into two stable products P1 and P2 have been formed on the acid hydrolysis of the irreversible process. The base hydrolysis process of the reversible reaction mechanism on the cysteine proteases inhibitors,

results in the formation of a stable intermediate INT2, which has been formed through the transition state TS4. The numerical frequency calculation has also confirmed this TS4 state. During the formation of the TS4, the bond length of C_1–O_7, C_8–O_{10} and C_{27}–N_{28} gets elongated and the values are found to be 0·010, 0·007 and 0·006 Å at B3PW91/6-31 + G* level of the theory respectively. At the same time, the bond between C_{12}–C_{13}, C_{12}–O_{14} and C_{26}–C_{27} atoms are shortened whose values are found to be 0·015, 0·186 and 0·007 Å at B3LYP/6-31 + G* level of theory respectively. During the formation of transition state TS4, the bond between O_{14}–H_{25} atoms at INT1 gets cleaved on hydrolysis, meanwhile an electron shift occurred between O_{14}–H_{25}, and O_{14}–C_{12} bonds. Due to this electron shift, the σ bond character between C_{12}–O_{14} atoms once again changed to a π bond character. The bond length between C_{12}–O_{14} atoms gets contract and the values are found to be 0·199 and 0·191 Å at B3LYP and B3PW91/6-31 + G* levels of theory. At the same time, the loosely bonded S_{24}–C_{14} atoms gets cleaved; once again the loosely bonded cysteine enzyme S^- ions get separated from acylhydroximate carbon atom C_{14} and bind with H^+ ion. The energy barrier between the INT1 and TS4 is found to be 76·44, 76·40 and 76·23 kcal/mol at the above levels of theory. The occurrences of the high energy barrier between INT1 and TS4 states might be due to the hydrolysis with water molecule.

The entire intramolecular hydrogen bonded networks C_2–H_5…O_{31} and C_{26}–H_3...O_{10} of INT1 are cleaved in order to form a new intermolecular hydrogen bond on N_{28}–H_{35}…O_{10} atoms at TS4 and the stabilization energy of N_{28}–H_{35}…O_{10} is found to be 3·27 kcal/mol at B3LYP/6-31+G* level of theory. During the formation of INT2, the bond length C_1–O_7, C_{12}–O_{14} and S_{24}–H_{25} get contracted and the contracted values are found to be 0·014, 0·014 and 0·002 Å at the B3PW91/6-31+G* level of theory. The intermolecular hydrogen bonds N_{28}–H_{35}…O_{10} and C_{26}–H_{33}…O_{10} are observed at INT2, and the stabilization energies are found to be 2·90 and 1·02 kcal/mol at B3LYP/ /6-31+G* level of theory. The energy barrier between TS4 and INT2 is found to be 6·26, 6·704 and 6·46 kcal/mol at B3LYP/6-31+G*, B3PW91/6-31+G* and MP2//B3LYP/6-31+G* levels of theory respectively.

Table 6. Calculated energy barrier (kcal/mol) for the reaction mechanism of cystein with *O*-acyl hydroxamates at DFT and *ab initio* methods implementing 6-31 + G* basis set.

System	B3LYP	B3PW91	MP2
R–TS1	–15·24	–12·05	–4·07
TS1–INT1	1·79	1·53	0·12
INT1–TS2	51·86	50·81	42·23
TS2–P1	0·32	0·73	0·75
INT1–TS3	59·20	57·65	60·36
TS3–P2	5·52	0·65	5·25
TS4–INT2	6·23	6·70	6·46
INT2–TS5	20·56	20·63	18·23
TS5–P3	8·92	10·26	7·43

3.3a *Formation of P3:* During the oxidation of the intermediate INT2, the stable intermediate INT2 structure breaks down to form a product P3 through the transition state TS5. The numerical frequency calculation has confirmed this TS5 state. During the formation of product P3, an intermolecular transition has been occurred, in which the cysteine molecule, the S–H bond is once again deprotonated to form the stable product P3. While on the deprotonation, hydrogen atom H_{25} of the cysteine molecule was directed to the oxygen atom O_{10} and binds strongly with *O*-acylhydroxamate molecule. At the same time, the deprotonated enzymatic cysteine S^- ions bind once again to strong electrophile of *O*-acylhydroxamate carbon atom C_8. Meanwhile, the π bond character between O_{10}–C_8 atoms has been changed to σ bond character. The bond length between O_{10}–C_8 gets elongated and the values are found to be 0·187 and 0·177 Å at B3LYP/6-31 + G* and B3PW91/6-31 + G* levels of theory. The changes of the bonds are confirmed by the structural parameters (elongation of bond length) and topological analysis (low electron density at bond critical point). The energy barrier between INT2 and transition state TS5 is found to be 13·56, 20·63, and 10·23 kcal/mol at the above levels of theory respectively. During the oxidation of INT2, the entire intra-molecular and inter-molecular hydrogen bonds break down to form the stable product P3, also, the stability of the product P3 is low on comparing with the intermediate INT2. The variation of the stability might be due to the breakdown of all intra-molecular and inter-molecular hydrogen bonded networks. The energy barrier between INT2 and the product P3 is found to be 20·48, 30·89 and 19·40 kcal/mol at B3LYP/6-31 + G*, B3PW91/6-31 + G* and MP2//B3LYP/6-31 + G* levels of theory respectively. At product P3, the bond between cysteine and *O*-acylhydroxamate C_8–S_{24} atoms is strong which shows the inhibiting nature of the

product P3. The energy barrier between the TS5 and P3 is found to be 6·92, 10·26 and 9·17 kcal/mol at B3LYP/6-31 + G*, B3PW91/6-31 + G* and MP2//B3LYP/6-31 + G* levels of theory respectively. The active enzymatic cysteine is completely changed to inactive form at product P3. The products P1, P2 and P3 are energetically more stable than the reactant and hence the reaction enthalpy is found to be exothermic. The product P3, when reduced by thiol, yields the intermediate INT2 once again, as a result of the reversible process.

4. Conclusion

In this article, we have studied the reaction mechanism of the cysteine proteases with *O*-acylhydroxamate using B3LYP/6-31 + G* and B3PW91/6-31 + G* levels of density functional theory and MP2//B3LYP/6-31 + G* level of *ab initio* theory in gas phase. After the breakdown of tetrahedral intermediate INT1, small 1–2 aniontropic has formed and re-arranged to give stable by-products sulfenamide P1 and thiocarbamate P2 with considerable energy loss. The energy barrier between the tetrahedral intermediate INT1 and product P1 is found be low when compared to that of the product P2, so it favours to the formation of the reaction steps resulting P1 and this result agrees with experimental process.[7] The strong binding nature of C_{12}–S_{24}, N_{11}–S_{24} and C_8–S_{24} bonds with P1, P2 and P3 of the reaction step shows the inhibiting nature of the *O*-acylhydroxamate with cysteine proteases. AIM analyses agree with the results. This theoretical calculation shows that, the tetrahedral intermediate structure is also a stable species (not TS structure) though it was not detected by any experimental techniques. The IRC calculations connect the transition state between R-INT1, INT1-P1 and INT1-P2. The reaction energy is found to be exothermic in the formation of product P1, P2 and P3. The stabilization energy of intra-molecular and inter-molecular hydrogen bonds in the reaction steps of cysteine with *O*-acylhydroxamate has been calculated using AIM and NBO analyses.

Acknowledgments

The authors are thankful to the Department of Science and Technology, Government of India for the financial assistance to create the Central Computer Lab under the DST–FIST Programme.

References

1. (a) Fersht A 1999 *Structure and mechanism in protein science. A guide to enzyme catalysis and protein folding* (New York: W.H. Freeman and Company) 2nd edn; (b) Jencks W P 1987 *Catalysis in chemistry and enzymology* (New York: Dover Publications)
2. Walkinshaw M D 1992 *Med. Res. Rev*. **12** 317
3. Dermuth H-U 1990 *J. Enzyme Inhib*. **3** 249
4. Hans-Ulrich Demuth, Angelika Schierhorn, Philip Bryan, Ralph Hofke, Heidrrum Kirschke and Dieter Bromme 1996 *Biochim. Biophys. Acta* **1295** 179
5. Rawlings N D and Barrett A J 1999 *Nucl. Acids Res*. **27** 325
6. McGrath M E 1999 *Ann. Rev. Biophys. Biomol Struct*. **28** 181
7. Hans-Hartwing Otto and Tanja Schirmeister 1997 *Chem. Rev*. **97** 133
8. Valerie J, Robinson J, Coles, Smith R A and Allen Krantz 1991 *J. Am. Chem. Soc*. **113** 7760
9. (a) Fischer G, Demuth H-U and Barth A 1983 *Pharmazie* **38** 249; (b) Demuth H-U, Neumann U, Schaper C, Fischer G and Barth A 1988 *J. Enzyme Inhib*. **2** 129
10. Bromme D, Fittkau S and Demuth H-U 1989 *J. Biochem*. **263** 861
11. Smith R A, Peter J, Coles, Spencer R W, Copp L J, Jones C S and Krantz, A 1988 *Biochem. Biophys. Res. Commun*. **155** 1201
12. Groutas W C, Stanga M A and Brubaker M J 1989 *J. Am. Chem. Soc*. **111** 1931
13. Marcin Hoffmann, Jacek Rrychlewski, Maria Chrzanowska and Tadeusz Hermann 2001 *J. Am. Chem. Soc.* **123** 6404
14. (a) Fuki K 1970 *J. Phys. Chem*. **74** 4161; (b) Ishida K, Morokuma K and Komornicki A 1977 *J. Chem. Phys.* **66** 2153
15. Cioslowski J 1994 *Chem. Phys. Lett*. 151
16. Carpenter J E and Weinhold F 1988 *J. Mol. Struct*. (*Theochem*) 1**69** 41; (Gledening E D, Reed A E, Carpenter J A and Weinhold F NBO Version 3.1)
17. Frisch M J *et al* 2001 Gaussian 98, Revision A.11.2, Pittsburgh PA, Gaussian, Inc
18. (a) Foresman J B, Frisch A 1996 *Exploring chemistry with electronic structure methods* Pittsburgh, P A: Gaussian. Inc; **(**b) Jensen F 1998 *Introduction to computational chemistry* (New York: Wiley)
19. Koch U and Popelier P LA 1995 *J. Phys. Chem*. **99** 9747
20. Popelier P L A and Bader R F W 1992 *Chem. Phys. Lett.* **189** 542
21. Perakyla M and Kollman P A 2000 *J. Am. Chem. Soc.* **122** 3436
22. Warshel A, Russell, 1986 *J. Am. Chem. Soc*. **108** 6569
23. Daggett V, Schroder S, Kollman P A 1991 *J. Am. Chem. Soc*. **113** 8926
24. Staton R V, Perakyla M, Bakowies D, Kollman P A 1998 *J. Am. Chem. Soc*. **120** 3448